Cone Penetration Testing 2022 – Gottardi & Tonni (eds)

CPTU-detection of thin clay layers in sand: Results from calibration chamber tests

H. Skrede
Norwegian Geotechnical Institute (NGI), Norwegian University of Science and Technology (NTNU), Norway

H.B. Hammer
Dr.techn. Olav Olsen AS, Norway

S. Nordal
Norwegian University of Science and Technology (NTNU), Norway

J.-S. L'Heureux
Norwegian Geotechnical Institute (NGI), Norway

ABSTRACT: The detection of thin clay layers (i.e. ≤ 20 cm) is challenging for all conventional geotechnical field investigations techniques, including high quality CPTU tests. During the last two years, a research program has been carried out in the geotechnical laboratory at NTNU in Trondheim. The work aims to identify possibilities and limitations in detecting thin clay layers and assess their properties using the CPTU tool. Tests were run in a pressurized chamber where thin horizontal clay layers of both pottery clay and natural, sensitive clay were embedded in a homogenous, medium dense sand. Both a standard piezocone (10 cm^2) and a mini-piezocone (5 cm^2) have been utilized. The results show to what degree the CPTU response in thin layers is influenced by the surrounding sand, and how this influence in practice may lead to serious overestimation of shear strength in thin layers. In addition, the effect of depth-offset of measurements in connection with soil type characterization was evaluated.

1 INTRODUCTION

Analyses of past landslides along the coast of Norway have shown that thin clay layers in sandy shoreline deposits often act as a sliding plane (L'Heureux et al. 2010). An example of a landslide that caused fatalities with these characteristics is the Finneidfjord landslide, which occurred in 1996 (Longva et al. 2003). The clay layers may be so thin (i.e. < 20 cm) that even high quality survey techniques, alike the CPTU, struggle to detect the layers.

This is the background of an ongoing research program at NTNU. A large-scale pressurized model testing facility has been set up and samples are built-in with clay layers of various thicknesses embedded in sand. CPTU-soundings are conducted on chamber samples with the aim of determining if thin layers can be properly identified, and to which degree it is possible to determine the properties of these layers. This article will mainly focus on the executed laboratory experiments and the most important results.

Similar research on the topic has been conducted by e.g. van der Linden et al. (2018) and de Lange et al. (2018), with main focus on liquefaction potential and pile resistance.

2 METHODOLOGY

In the research program at NTNU, six experiments have so far been conducted (E1-E6). Each experiment consists of constructing a chamber sample, pressurizing it, performing soundings on the chamber sample followed up by excavation with supplementary laboratory testing of soil properties. Clay type, layer thicknesses and stress levels have been systematically varied during the experimental program. This chapter describes the methodology in general, for further details it is referred to MSc theses of Skrede (2021) and Hammer (2020).

Chamber samples were built into a testing chamber of about 1.5 meter height, using reinforced concrete cylinders (sewage manhole rings) with an internal diameter of 1.2 meter. In the base of the chamber an outlet was installed to allow for regulation of the water level. A pore pressure sensor was installed on the outlet.

DOI: 10.1201/9781003308829-101

The bottom 10 cm of the chamber was filled with gravel, covered by a filter cloth. This allowed for an evenly distributed in and outflow of water across the chamber cross-section during the building procedure, preventing interior channelling in the sand. Above the filter cloth a first sand layer of 10 cm was built in. Pressure cells of the Geokon 3500-3 model were placed on top, four horizontally and one vertically (Figure 1). The cells were calibrated by inserting them into a special designed casing and imposing air pressure within the casing. Unfortunately, the cells suffered from some sensitivity drift. This was dealt with by correcting the data linearly from start to end.

The sand used in the chamber came from Kvål, with a d_{50} of 0.492 mm; C_u of 4.24; and e_{min} and e_{max} of respectively 0.502 and 0.873. Two types of clays were used in the tests. The first clay was an industrially made kaolin pottery clay (K148 by Sibelco) delivered in bricks (31x11x12cm^3). The second clay type was a natural sensitive clay extracted from 8 to 10,5 meters depth at Flotten, a Norwegian Geo-Test Site, sampled by using a mini-block sampler providing cylindrical samples with 16 cm diameter (Emdal, et al. 2016).

All the pottery clay bricks had almost identical properties. The very sensitive, quick clay extracted from Flotten, is well-documented based on-site investigations reported by L'Heureux et al. (2019). The key properties of the clays are presented in Table 1.

The procedure of constructing sand layers aimed at a homogeneous, medium densely packed sand (relative density D_r ~40-60%) in order to resemble a natural sand deposit. Details about the procedures are found in the MSc theses (Hammer, 2020; Skrede, 2021).

In all experiments except the last, pottery clay was utilized. From each brick of pottery clay a specimen was cut to a preferred dimension with a thread saw. Several specimens were then laid together side by side and carefully clamped to form a clay "unit". The purpose of uniting several specimens was to make the clay layer wide enough to act as if it was a continuous horizontal layer. It was still made with limited horizontal extension and did not cover the entire cross section of the chamber partly to save material, but primarily to allow water to flow vertically in the chamber during sample construction and testing.

In the last experiment (E6) mini-blocks (diameter of 16 cm) of natural sensitive clay from Flotten were utilized. Assemblance of units proved to be feasible also for the quick clay but required considerable precision and careful execution. Each clay layer was designed and placed so that the CPTU soundings would be close to the centre of the clay unit as illustrated in Figure 2 (layer set-up for tests E1-3 and E5).

Two penetrometers were utilized, firstly a standard sized (10 cm^2) NOVA-probe from GeoTech AB with a measurement frequency of about 1Hz. Secondly a mini electrical probe (5 cm^2) with an approximate measurement frequency of 8Hz that was kindly made available from Geomil Equipment B.V. This probe was exclusively used in the last experiment (E6). The rate

Table 1. Properties of pottery clay and clay from Flotten.

Parameter	Symbol	Pottery clay	Natural clay*	Unit
Water content	w	~24	~45	%
Liquid Limit	w_L	32.7	~28-33	%
Plastic limit	w_P	18.8	~20	%
Plasticity index	I_P	13.9	~8-13	%
Liquidity index	I_L	0.4	~2.4	-
Sensitivity	S_t	~2.5	50-350	-
Undrained shear strength	$s_{u,CAUC}$	27.5	~75	kPa

* Rough, values based on range of results around 8-10 m depth.

Figure 1. Pressure cell arrangement.

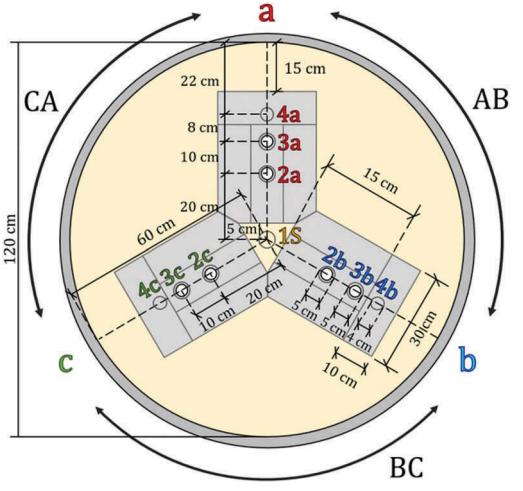

Figure 2. Cross-section of chamber with dimensions of both the clay set-up from experiment 1-3 and 5; and of the overlaying metal disc with its 10 soundings holes (1S, 2a-4c). Each of the 3 clay units shown here in grey are built from 4 specimens cut from bricks of pottery clay.

of penetration was set to 15 mm/s for all experiments to increase the spatial resolution, thus providing more continuous curves, still operating in accordance with European standard (EN ISO 22476-1:2012).

Further details about the chamber sample set-ups, and about how the signal processing was done to increase precision are found in the master's thesis (Skrede, 2021).

To simulate stress states at larger depths, the surface of the chamber samples was subjected to an over-burden load. The vertical stresses were imposed by a circular metal disc pushed down by three air-bellows fastened to an upper supporting metal framework, see Figure 3.

The chamber was designed with ten possible positions for CPTU testing. Three in-line holes were placed in 3 radial sectors 120 degrees apart, denoted sectors a, b, c. The centre hole is referred to as the S position. The holes were in addition numbered from the centre as 1,2,3 and 4. Thus position 1S is in centre while 4c is closest to the concrete wall in sector c. The reference system is shown in Figure 2. Multiple test positions were used for each chamber sample, these were divided into two rounds consisting of "primary soundings" and "secondary soundings". The primary soundings consisted of tests with significant distance to walls and previously tested positions. These were thus considered to reflect undisturbed soil. Secondary soundings were run after the primary soundings in neighbouring positions as reserve for validation, though the measurements reflect disturbed soil.

For each chamber sample, after CPTU testing, a meticulous excavation phase followed, where lab tests were conducted on both the clay and the sand to analyse the soil profile for density and strength.

3 THEORETICAL BACKGROUND

3.1 *Stress state in chamber – The silo effect*

The stress level in the chamber was influenced by the silo effect or the arching effect caused by vertical shear stresses on the wall. The formula by Janssen (1895) was used with effective stress parameters, Equation (1), to quantify the effect. The decay length, l', was estimated using the given surcharge, q; and the earth pressure cells at the base, to determine the stress $\sigma'_v(z)$ over the height of the chamber.

$$\overline{\sigma'_v(z)} = \gamma' l' + e^{-\frac{z}{l'}}(q - \gamma' l') \quad (1)$$

3.2 *CPTU-parametrizations*

The conventional procedure to classify soils from CPTU results is to normalize the corrected tip resistance, q_t, the sleeve friction, f_s, and the pore pressure, u_2 with respect to in-situ stress. This provides the normalized tip resistance, Q_t, the normalized friction ratio, F_r, and the pore pressure ratio, B_q; In Equations (2)-(4) q_n is the net cone resistance, see Equation (5).

$$Q_t = \frac{q_n}{\sigma'_{v,0}} \quad (2)$$

$$F_r = \frac{f_s}{q_n} \cdot 100\% \quad (3)$$

$$B_q = \frac{\Delta u_2}{q_n} \quad (4)$$

$$q_n = q_t - \sigma_{v,0} \quad (5)$$

Figure 3. The overburden loading framework on the chamber. Above: the actuator and the probe fixed to a framework.

To estimate the undrained shear strength, s_u, in the clay layers, the empirical relations suggested by Karlsrud et al. (2005) have been used, see Equations (6)-(8). The cone factors, N_i, in these formulas are based on OCR, S_t and I_P. These parameters were estimated for each specimen by using interpolated data from the Flotten site report (L'Heureux et al. 2019).

$$s_{u,kt} = \frac{q_n}{N_{kt}} \quad (6)$$

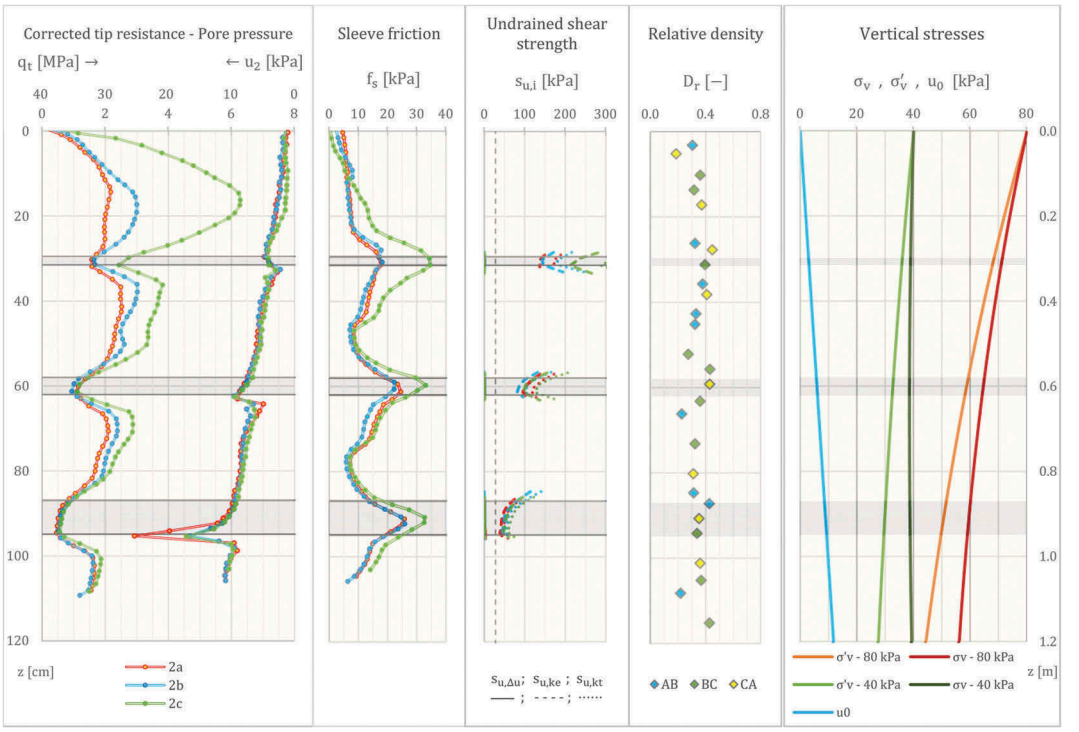

Figure 4. Experiment 5. Left: CPTU-measurements. Mid: Shear strength estimations for the clay layers, note that $s_{u,\Delta u}$ is approximately zero for all layers. Right: Sand density samples results and estimated stress distributions.

$$s_{u,\Delta u} = \frac{\Delta u_2}{N_{\Delta u}} \tag{7}$$

$$s_{u,ke} = \frac{q_t - u_2}{N_{ke}} \tag{8}$$

4 RESULTS

4.1 *Soundings from experiment 5*

The results of experiment 5 (Figure 4) illustrates typical trends that unveiled upon penetrating clay layers interbedded in sand. The clay layer thicknesses were respectively 2, 4 and 8 cm from the top. The surcharge was set to 40 kPa for soundings in holes 2a and 2b, 80 kPa for 2c. These were the primary soundings, while secondary soundings were performed in the number 3 holes. The latter are not presented in this figure.

The u_2-measurements were depth-shifted to account for the distance between the position of the pore pressure sensor and the cone tip (the depth of q_t), while f_s was corrected to the end of the sleeve closest the tip, see ch. 5.2 for explanation. The sample preparation was quite successful in experiment 5 with a fairly constant relative density, D_r, in the sand over the depth of the chamber. Comparing various tests, it is confirmed that q_t varies considerably with relative density and stress level.

4.2 *Normalized profiles*

To study the variation of q_t through layers of varying thicknesses, a compilation of q_t-profiles is shown in Figure 5. The depth has been normalized with respect to the cone diameter, d_c. The q_t-profiles in the graphs are indexed X-Y-Z for respectively experiment number; surcharge on top of chamber sample in kPa; and sounding hole. The colour of the profiles is according to the surcharge level, with primary and secondary soundings respectively solid and dashed. The jagged appearance of the mini-cone profiles is due to the different approach used in post data treatment for the mini cone. The profiles include a penetration through a 36 cm high pottery clay unit as a reference for the characteristic tip resistance, q_t^{char}, of the pottery clay (E4-40-3b). Here q_t^{char} is defined as the expected tip resistance in an infinitely thick layer for the specific stress level.

5 DISCUSSIONS

5.1 *The thin layering effect*

To what degree the measured q_t in the thin layers is higher than q_t^{char} depends on the ratio of the layer thickness over the cone diameter, H/d_c, and on the contrast between q_t^{char} in the clay and the tip resistance in the sand. The effect H/d_c is shown in Figure 5 where the mini-cone profiles from E6: 4b and 4c have equal sensing- and developing depths compared to the standard-cone profile 1S, when normalized. The "depth terms", sensing- and developing depths, denote respectively the distance ahead of an interface where q_t is influenced by the next layer; and the distance after the interface q_t retain influence from the previous layer.

The test results show that the q_t-profiles through interbedded layers are not symmetric, as the developing- and sensing distances are different for the upper and lower interface of each clay layer, as apparent in Figure 4 and Figure 5. The characteristics of q_t-profiles during transitions thus have some degree of uniqueness, which then might be used in an attempt to back-calculate layer thicknesses and q_t^{char}.

The tip resistance approaches the characteristic value asymptotically with increasing interbedded layer thicknesses. This implies that calculated s_u based on Equation (6) and (8) provide overestimations of the "true s_u" (i.e. s_u based on triaxial CAUC-test) whenever the developing depth is not surpassed. As to illustrate, overestimation magnitudes (with reference to calculated extremal value) are listed for all experiments on pottery clay in Table 2. The table does in addition include the magnitude of underestimation when calculated s_u is based on Equation (7), which is a consequence of the excess pore pressure build-up never approaching the characteristic value. From the reference test (E4-40-3b), the developing depth of q_t was about 5-5.3 d_c (18-19 cm) after the interface.

Table 2. The ratios between the extremal value of the CPTU-s_u-parametrizations within a clay layer compared to the "true s_u" of the clay, presented for different clay layer thicknesses. For $s_{u,kt}$ and $s_{u,ke}$ the ratio of overestimation is presented, while for $s_{u,\Delta u}$ the ratio of underestimation is presented.

Layer thickness	2 cm	4cm	8cm	12 cm
$s_{u,kt,min}/s_u$	6.3-10.5	2.3-4.6	1.4-2.1	1.1
$s_{u,ke,min}/s_u$	5.0-7.7	2.0-3.5	1.3-1.7	0.9-1.0
$s_u/s_{u,\Delta u,max}$	80-125	35-65	4-25	1.8-3.4

5.2 *Depth offset*

During penetration through thin layers of clay, all CPTU-parameters starts to approach their characteristic value, yet these approaches are "cancelled" upon closing in on the second interface. As measurements are saved as data points versus time, the measurements from the pore pressure sensor are actually made about 1 cone diameter behind the cone tip. This means that the extremal value of u_2 is saved at a different depth than the extremal value of q_t, consequently lowering the extremal value of the pore pressure ratio, B_q, see Figure 6. For the soundings on the natural sensitive clay (E6-1S;4b;4c), the effect of correcting the depth-offset altered the B_q extremal value up to 0.15. Moreover, due to the short distances of excess pore pressure build-up in thin layers, B_q never approach levels which are close to the reference values, requiring extra care upon interpreting CPTU.

Accounting for the depth-offset is more complicated for the sleeve friction measurements, as each measurement is the product of stresses working on the entire friction sleeve. Therefore, it can be stated that the sleeve's length entails a smoothening effect, making it a component of less depth accuracy and maybe relevance regarding transitions. However, from the experiments, a consistent pattern is apparent: As the probe transits from the sand to the clay the sleeve friction increases drastically when the front end of the sleeve hits the original level of the interface (prior to deformation), whereupon it is decreasing (ref. E4-40-3b). Due to this phenomenon f_s may turn out to be quite useful for identifying thin layers of clay embedded in sand. However, this part is associated with great uncertainty as field measurements of f_s can be rather high in sand, while low in clay, and in addition, f_s varies a lot with probe types. Consequently, this aspect requires further research.

With regards to the previous paragraph, the choice of depth correction for f_s is not obvious. Upon correcting the data points upwards on the sleeve, the extremal magnitude of F_r is smoothened with respect to both lower and upper bounds, making a distinction between materials more difficult (Figure 7). Ironically and conceptually incorrect, the greatest magnitude of F_r is reached if no corrections are made at all.

In conclusion, depth-offset has a big impact on the classification parametrizations during transitions, greatly impacting the identification of the materials

and the layer thicknesses. It should however be underlined that offset corrections do not influence s_u -estimations except for $s_{u,ke}$ with a negligible magnitude.

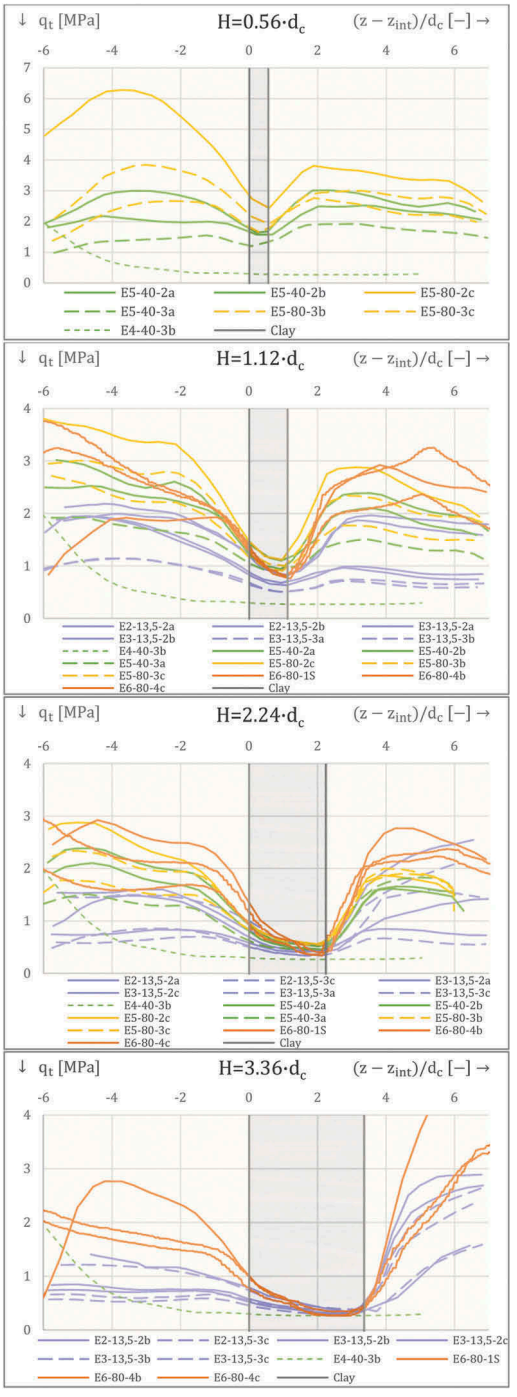

Figure 5. Rotated tip resistance profiles of penetration of clay layers (surface towards left, chamber base towards right), normalized with respect to the cone diameters. The thicknesses of the layers penetrated by respectively the standard cone and the mini-cone were 2, 4, 8 and 12 cm; and 2.8, 5.7 and 8.5 cm. Soundings in natural sensitive clay are marked with orange (E6).

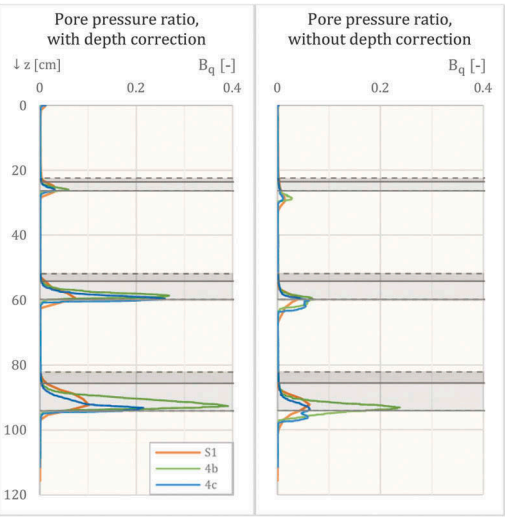

Figure 6. Relative difference of B_q when depth-offset is corrected (left), and not corrected (right) (E6-1S;4b;4c).

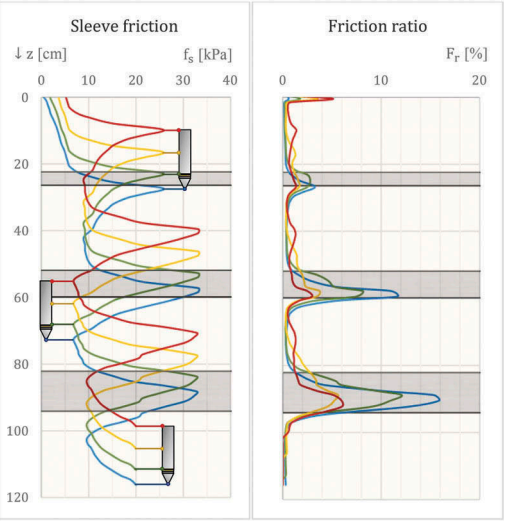

Figure 7. Left: Profile with f_s-readings (E6-1S) not corrected with respect to depth offset (blue) and profiles adjusted for different positions on the friction sleeve. Right: Resulting F_r-graphs based on data from the graphs in the left profile.

6 CONCLUSIONS

Thin, weak and possibly sensitive interbedded clay layers are not easily detected as characteristic reference values are not reached before the cone leaves the layer. In this respect, depth correction proves to be very important for the magnitude of the normalized ratios F_r

and B_q. Furthermore, calculations of s_u based on the correlations $s_{u,kt}$ and $s_{u,ke}$ will lead to overestimation of s_u as the recorded tip resistance does not approach the characteristic tip resistance of the thin layer. Likewise, calculation of s_u based on the correlation $s_{u,\Delta u}$ will lead to severe underestimation due to the small excess pore pressure build-up in thin layers.

ACKNOWLEDGEMENTS

The authors would like to acknowledge everyone who have contributed to this research program, mainly lab staff at NTNU. We are grateful to NGI for financially aiding the program and to Geomil Equipment for generously lending the mini-cone to the research.

REFERENCES

Emdal, A., Gylland, A., Amundsen, H.A., Kåsin, K., Long, M. 2016. Mini-block sampler. *Canadian geotechnical journal*, 53(8):1235–1245. https://cdnsciencepub.com/doi/10.1139/cgj-2015-0628

Hammer, H.B. 2020 *Physical experiments on CPTU thin-layer effects of thin clay layers embedded in sand: With analysis-and possible correction of cone resistance in layered profiles*. M.Eng. Master Thesis. Faculty of Civil Engineering, Norwegian University of Science and Technology (NTNU). https://ntnuopen.ntnu.no/ntnu-xmlui/handle/11250/2689484

Janssen, H.A. 1895. Versuche über Getreidedruck in Silozellen. *Zeiteschrift des Vereins deutscher Ingenieure*. 39 (35):1045–1049. https://web.archive.org/web/20110303223406/http:/www.phy.duke.edu/~msperl/Janssen/Janssen1895.pdf

Karlsrud, K., Lunne, T., Kort, D.A., Strandvik, S. 2005. CPTU correlations for clays. *In Proceedings of the international conference on soil mechanics and geotechnical engineering*, 2005, Osaka,16:693–702. https://www.issmge.org/publications/publication/cptu-correlations-for-clays

de Lange, D.A., Terwindt, J. and van der Linden, T.I. 2018. CPT in thinly inter-layered soils. Paper presented at the Cone Penetration Testing 2018: *Proceedings of the 4th International Symposium on Cone Penetration Testing (CPT'18)*, 21-22 June, 2018, Delft, The Netherlands. https://www.icevirtuallibrary.com/doi/10.1680/jgeen.17.00061

L'Heureux, J. S., Hansen. L., Longva, O., Emdal, A., & Grande, L. O. 2010. A multidisciplinary study of submarine landslides at the Nidelva fjord delta, Central Norway, - Implications for the assessment of geohazards. *Norwegian Journal of Geology*, Vol 90: 1–20.Trondheim, ISSN 029-196X. https://www.researchgate.net/publication/234101112_A_multidisciplinary_study_of_submarine_landslides_at_the_Nidelva_fjord_delta_Central_Norway_-_Implications_for_geohazard_assessment

L'Heureux, J.S., Lindgård, A., Emdal, A. 2019. The Tiller-Flotten research site: Geotechnical characterization of a very sensitive clay deposit. *AIMS Geosciences*, 5(4):831–867. https://ngi.brage.unit.no/ngi-xmlui/handle/11250/2630879

Longva O., Janbu N., Blikra L.H., Bøe R. 2003. The 1996 Finneidfjord Slide: Seafloor Failure and Slide Dynamics. In: Locat J., Mienert J., Boisvert L. (eds.), Submarine Mass Movements and Their Consequences. *Advances in Natural and Technological Hazards* Research, *vol 19*. Springer, Dordrecht. https://link.springer.com/chapter/10.1007/978-94-010-0093-2_58

Skrede, H. 2021 *CPTU-detection of thin clay layers in sand: Results from calibration chamber testing*. M.Eng. Master Thesis. Faculty of Civil Engineering, NTNU. https://ntnuopen.ntnu.no/ntnu-xmlui/handle/11250/2977001

van der Linden, T.I., De Lange, D.A., & Korff, M. 2018. Cone Penetration Testing in Thinly Inter-Layered Soils. *Geotechnical Engineering*. https://www.taylorfrancis.com/chapters/oa-edit/10.1201/9780429505980-51/cpt-thinly-inter-layered-soils-de-lange-terwindt-van-der-linden

European committee for standardization. 2012. *Geotechnical investigation and testing: Field testing: Part 1: Electrical cone and piezocone penetration test*. EN ISO 22476-1: 2012.